Observation of Phase Separation in a Strongly Interacting Imbalanced Fermi Gas

Y. Shin,* M. W. Zwierlein, C. H. Schunck, A. Schirotzek, and W. Ketterle

Department of Physics, MIT-Harvard Center for Ultracold Atoms, and Research Laboratory of Electronics, Massachusetts Institute of Technology, Cambridge, Massachusetts, 02139, USA

(Received 15 June 2006; published 18 July 2006; corrected 21 July 2006)

We have observed phase separation between the superfluid and the normal component in a strongly interacting Fermi gas with imbalanced spin populations. The *in situ* distribution of the density difference between two trapped spin components is obtained using phase-contrast imaging and 3D image reconstruction. A shell structure is clearly identified where the superfluid region of equal densities is surrounded by a normal gas of unequal densities. The phase transition induces a dramatic change in the density profiles as excess fermions are expelled from the superfluid.

DOI: 10.1103/PhysRevLett.97.030401 PACS numbers: 03.75.Ss, 03.75.Hh, 05.70.Fh

Cooper pairing is the underlying mechanism for the Bardeen-Cooper-Schrieffer (BCS) superfluid state of an equal mixture of two fermionic gases. An interesting situation arises when the two components have unequal populations. Does the imbalance quench superfluidity, does it lead to phase separation between a balanced and an imbalanced region, or does it give rise to new forms of superfluidity? A search for exotic superfluid states is promising in imbalanced mixtures, since the imbalance destabilizes BCS-type s-wave pairing, which is usually the strongest pairing mechanism [1–4]. Recently, this problem has been experimentally addressed in ultracold atomic Fermi clouds with controlled population imbalances [5–7]. Superfluidity was observed in a strongly interacting regime with a broad range of imbalances, and the Clogston limit of superfluidity [8] was characterized [5,7].

The phase separation scenario suggests that unpaired fermions are spatially separated from a BCS superfluid of equal densities due to the pairing gap in the superfluid region [9–11]. In our previous experiments [5,7], we observed a strong central depletion in the difference profiles of expanding clouds indicating that excess atoms are expelled from the superfluid region. Reference [6] reports depletion of excess atoms at the trap center. None of these experiments answered the questions of whether the densities of the two spin components are *equal* in the *superfluid* region and whether phase separation or rather distortions of the cloud due to interactions have occurred [12,13].

Here we report the direct observation of phase separation between the superfluid and the normal region in a strongly interacting Fermi gas with imbalanced spin populations. The density difference between the two spin components is directly measured *in situ* using a special phase-contrast imaging technique and 3D image reconstruction. We clearly identify a shell structure in an imbalanced Fermi gas where the superfluid region of equal densities is surrounded by a normal gas of unequal densities. This phase separation is observed throughout the strongly interacting regime near a Feshbach resonance. Furthermore, we characterize the normal-to-superfluid phase transition of an imbalanced Fermi mixture using *in situ* phase-contrast imaging. The onset of superfluidity induces a dramatic change in the density profiles as excess fermions are expelled from the superfluid.

A degenerate Fermi gas of spin-polarized ^{6}Li atoms was prepared in an optical trap after laser cooling and sympathetic cooling with sodium atoms [14,15]. The population imbalance δ of the two lowest hyperfine states $|1\rangle$ and $|2\rangle$ was adjusted with a radio-frequency sweep [5]. Here $\delta \equiv (N_1 - N_2)/(N_1 + N_2)$, where N_1 and N_2 are the atom numbers in $|1\rangle$ and $|2\rangle$, respectively. Interactions between these two states were strongly enhanced near a broad Feshbach resonance at $B_0 = 834$ G. The final evaporative cooling was performed at $B = 780$ G by lowering the trap depth. Subsequently, the interaction strength was adiabatically changed to a target value by adjusting the value of the magnetic-bias field B with a ramp speed of ≤ 0.4 G/ms. For typical conditions, the total atom number was $N_t = N_1 + N_2 \approx 1 \times 10^7$ and the radial (axial) trap frequency was $f_r = 130$ Hz ($f_z = 23$ Hz).

The condensate fraction in the imbalanced Fermi mixture was determined via the rapid transfer technique [16,17]. Immediately after turning off the trap, the magnetic field was quickly ramped to $B = 690$ G ($1/k_F a \approx 2.6$, where k_F is defined as the Fermi momentum of a noninteracting equal mixture with the same total atom number and a is the scattering length) in approximately 130 μs. The density profile of the expanding minority cloud was fit by a Gaussian for normal components (thermal molecules and unpaired atoms) and a Thomas-Fermi (TF) profile for the condensate [18].

The density difference between the two components was directly measured using a phase-contrast imaging technique (Fig. 1). In this imaging scheme, the signs of the phase shifts due to the presence of atoms in each state are opposite so that the resulting phase signal is proportional to the density difference n_d of the two states [19]. This technique allows us to directly image the *in situ* distribution of the density difference $n_d(\vec{r})$ and avoid the shortcoming of previous studies [5–7] where two images were subtracted from each other.

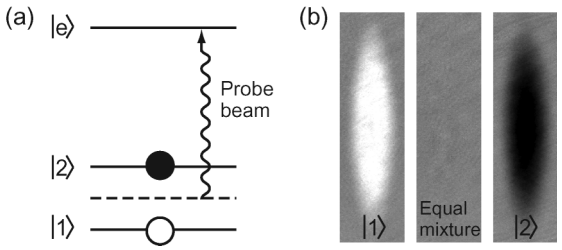

FIG. 1. Phase-contrast imaging of the density difference of two spin states. (a) The probe beam is tuned to the red for the $|1\rangle \rightarrow |e\rangle$ transition and to the blue for the $|2\rangle \rightarrow |e\rangle$ transition. The resulting optical signal in the phase-contrast image is proportional to the density difference $n_d \equiv n_1 - n_2$, where n_1 and n_2 are the densities of the states $|1\rangle$ and $|2\rangle$, respectively. (b) Phase-contrast images of trapped atomic clouds in state $|1\rangle$ (left) and state $|2\rangle$ (right) and of an equal mixture of the two states (middle).

For a partially superfluid imbalanced mixture, a shell structure was observed in the *in situ* phase-contrast image (Fig. 2). Since the image shows the column density difference (the 3D density difference integrated along the y direction of the imaging beam), the observed depletion in the center indicates a 3D shell structure with even stronger depletion in the central region. The size of this inner core decreases for increasing imbalance, and the core shows a distinctive boundary until it disappears for large imbalance. We observe this shell structure even for very small imbalances, down to 5(3)%, which excludes a homogeneous superfluid state at this low imbalance, contrary to the conclusions in Ref. [6].

The reconstructed 3D profile of the density difference shows that the two components in the core region have equal densities. We reconstruct 3D profiles from the 2D distributions $\tilde{n}_d(x, z)$ of the column density difference using the inverse Abel transformation (Fig. 3) [20]. The reconstruction does not depend on the validity of the local density approximation (LDA) or a harmonic approximation for the trapping potential [12,21,22] and assumes only cylindrical symmetry of the trap. The two transverse trap frequencies are equal to better than 2% [15]. A 1D profile obtained by integrating $\tilde{n}_d$ along the axial direction [Fig. 3(d)] shows a flattop distribution, which is the expected outcome for a shell structure with an empty inner region in a harmonic trap and assuming LDA.

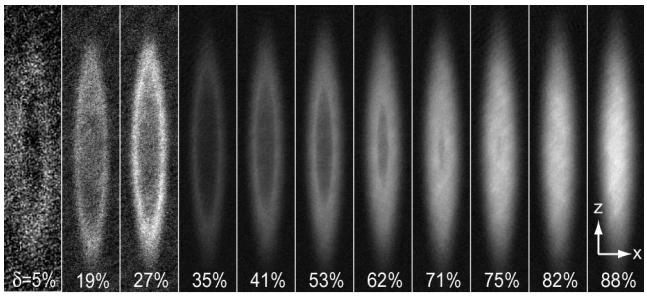

FIG. 2. *In situ* direct imaging of trapped Fermi gases for various population imbalance δ. The integrated 2D distributions of the density difference $\tilde{n}_d(x, z) \equiv \int n_d(\vec{r})dy$ were measured using phase-contrast imaging at $B = 834$ G for total atom number $N_t \approx 1 \times 10^7$. For $\delta \leq 75\%$, a distinctive core was observed showing the shell structure of the cloud. The field of view for each image is 160 μm $\times$ 800 μm. The three leftmost images are displayed with different contrast levels for clarity. The image with $\delta = 5(3)\%$ was taken for $N_t \approx 1.7 \times 10^7$.

The presence of a core region with equal densities for the two components was correlated with the presence of a pair condensate. The density difference at the center n_{d0} along with the condensate fraction is shown as a function of the imbalance δ in Fig. 4. As shown, there is a critical imbalance δ_c where superfluidity breaks down due to large imbalance [5,7]. In the superfluid region, i.e., $\delta < \delta_c$, n_{d0} vanishes, and for $\delta > \delta_c$, n_{d0} rapidly increases with a sudden jump around $\delta \approx \delta_c$. We observe a similar behavior throughout the strongly interacting regime near the Feshbach resonance, $-0.4 < 1/k_F a < 0.6$. This observation clearly demonstrates that for this range of interactions a paired superfluid is spatially separated from a normal component of unequal densities.

The shell structure is characterized by the radius of the majority component, the radial position R_p of the peak in $n_d(\vec{r})$, the size R_c of the region where n_d is depleted, and the "visibility" α of the core region (Fig. 5). The sudden drop of α around $\delta \approx \delta_c$ results from the sudden jump of n_{d0}. The comparison between R_p and R_c shows that the boundary layer between the superfluid and the normal region is rather thin. It has been suggested that the detailed shape of profiles in the intermediate region could be used to identify exotic states such as the Fulde-Ferrell-Larkin-Ovchinnikov state [23–25]. This will be a subject of future research.

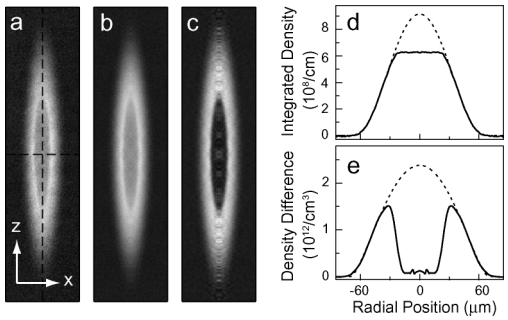

FIG. 3. Reconstruction of 3D distributions from their integrated 2D distributions. (a) An integrated 2D distribution $\tilde{n}_d$ with $\delta = 58\%$ at $B = 834$ G. (b) A less noisy distribution was obtained by averaging four quadrants with respect to the central dashed lines in (a). (d) The 1D profile obtained by integrating the averaged distribution along the z direction shows the "flattop" feature. (c) The 2D cut $n_d(x, y = 0, z)$ of the 3D distribution $n_d(\vec{r})$ was reconstructed by applying the inverse Abel transformation to (b). (e) The radial profile of the central section of the reconstructed 3D distribution in the xy plane. The dashed lines in (d) and (e) are fits to the profiles' wings using a TF distribution.

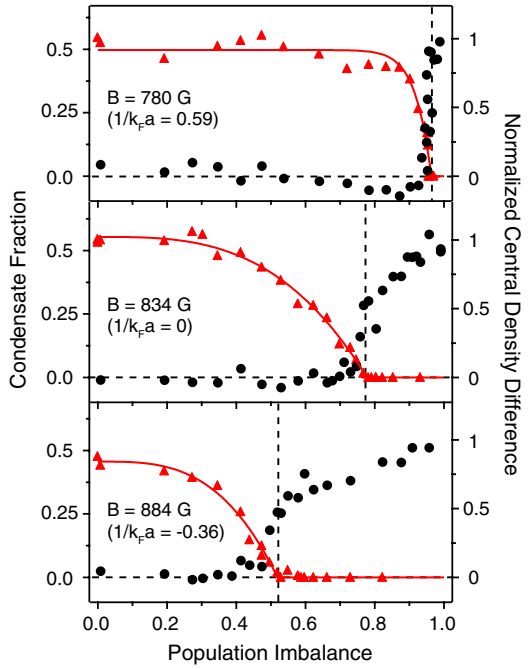

FIG. 4 (color online). Phase separation in a strongly interacting Fermi gas. Normalized central density difference η (black circles) and condensate fraction (red triangles) as functions of imbalance δ for various interaction strengths at our lowest temperatures ($T \lesssim 0.06T_F$). $\eta \equiv n_{d0}/n_0$, where n_{d0} was measured as the average over the central region of 7 μm $\times$ 40 μm in a 2D cut of the 3D distribution [Fig. 3(c)] and $n_0 = 3.3 \times 10^{12}$ cm^{-3} is the calculated central density of a fully polarized Fermi gas with $N_t = 1 \times 10^7$. The condensate fraction was determined from the minority component (see the text). The solid line is a fit for the condensate fraction to a threshold function $\propto (1 - |\delta/\delta_c|^n)$. The critical imbalances δ_c indicated by the vertical dashed lines were 96% (exponent $n = 21$), 77% ($n = 3.1$), and 51% ($n = 3.4$) for $B = 780$ G, $B = 834$ G, and $B = 884$ G, respectively.

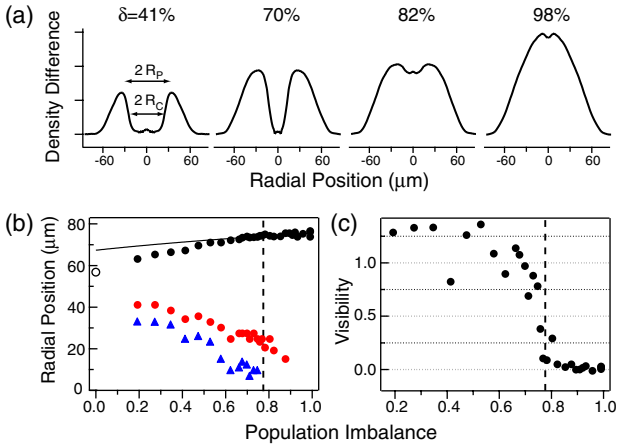

FIG. 5 (color online). Characterization of the shell structure. (a) Reconstructed 3D radial profiles at $B = 834$ G. (b) Radius of the majority component R (black circles), peak position of the density difference R_p (red circles), and radius of the empty core R_c (blue triangles) as a function of population imbalance δ. R was determined from the profiles' wings using a fit to a zero-temperature TF distribution. The solid line indicates the TF radius of the majority component in an ideal noninteracting case. R at $\delta = 0$ (open circle) was measured from an image taken with a probe frequency preferentially tuned to one component. R_c is defined as the position of the half-peak value in the empty core region for $\delta < \delta_c$. (c) Visibility of the core region is defined as $\alpha \equiv (n_d(R_p) - n_{d0})/(n_d(R_p) + n_{d0})$. For low δ, $n_d(R_p)$ is small, and small fluctuations of n_{d0} around zero lead to large fluctuations in α.

The superfluid requires equal central densities in the strongly interacting regime at our coldest temperatures. A normal imbalanced Fermi mixture will have unequal densities. Thus, one should expect that a visible change in the density difference occurs as the temperature is lowered across the normal-to-superfluid phase transition [7,9]. *In situ* phase-contrast images of a cloud at various temperatures are shown in Fig. 6. The temperature T of the cloud is controlled with the final value of the trap depth in the evaporation process. The shell structure appears and becomes prominent when T decreases below a certain critical value. This shell structure gives rise to the bimodal density profile of the minority component that we observed after expansion from the trap in our recent work [7]. Here we show via *in situ* measurements that the onset of superfluidity is accompanied by a pronounced change in the spatial density difference.

The phase transition is characterized in Fig. 7. As T is lowered, n_{d0} gradually decreases from its plateau value and the condensate fraction starts to increase. From the point of condensation (condensate fraction >1%) and deformation of the minority clouds [χ^2 in Fig. 7(b)], we determine the critical temperature $T_c = 0.13(2)T_F$ for the imbalance of $\delta = 56(3)\%$. $T_F = 1.7$ μK is the Fermi temperature of a noninteracting equal mixture with the same total atom number. The rise in χ^2, the drop in n_{d0}, and the onset of

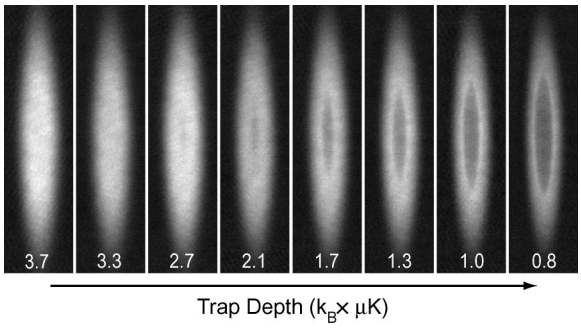

FIG. 6. Emergence of phase separation in an imbalanced Fermi gas. The temperature of the cloud was controlled by varying the final value of the trap depth U_f in the evaporation process. Phase-contrast images were taken after adiabatically ramping the trap depth up to $k_B \times 3.7$ μK ($f_r = 192$ Hz). The whole evaporation and imaging process was performed at $B = 834$ G ($N_t \approx 1.7 \times 10^7$, $\delta \approx 56\%$). The field of view for each image is 160 μm $\times$ 940 μm. The vertical and the horizontal scale of the images differ by a factor of 1.5.

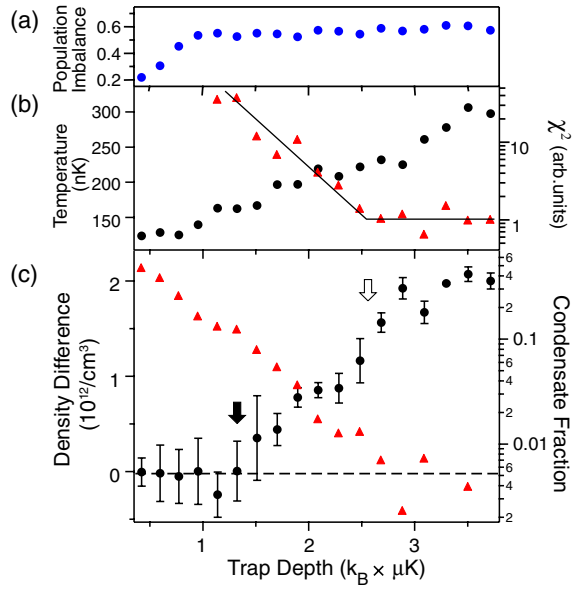

FIG. 7 (color online). Phase transition in an imbalanced Fermi gas. The phase transition shown in Fig. 6 was characterized by measuring (a) population imbalance δ, (b) temperature T (black circles), χ^2 for fitting the minority cloud with a finite temperature Fermi-Dirac distribution (red triangles), (c) central density difference n_{d0} (black circles), and condensate fraction (red triangles). The solid line is a guide to the eye for χ^2. δ decreased mainly due to loss in the majority component, which was reduced by 14% between $U_f/k_B = 3$ and 1 μK and more rapidly below 1 μK. The number of minority atoms was almost constant ($N_2 \approx 3.7 \times 10^6$). T was determined from the noninteracting outer region of the majority cloud after 10 ms of ballistic expansion [7]. T and n_{d0} are averaged values of three independent measurements. The open (solid) arrow in (c) indicates the position for T_c (T^*). See the text for the definitions of T_c and T^*.

condensation are all observed at about the same temperature. Better statistics are needed to address the question of whether some weak expulsion of majority atoms from the center occurs already slightly above T_c.

Below a certain temperature T^*, n_{d0} reaches zero while the condensate fraction is still increasing, implying that the superfluid region of equal densities continues to expand spatially with decreasing T (see Fig. 6). Full phase separation does not occur until this temperature $T^* < T_c$ is reached. We interpret the state between T^* and T_c as a superfluid of pairs coexisting with polarized quasiparticle excitations. This is expected, since at finite temperatures the BCS state of an equal mixture can accommodate excess atoms as fermionic quasiparticle excitations [23,26–28]. There is a finite energy cost given by the pairing gap $\Delta(T)$ for those quasiparticles to exist in the superfluid. The assumption that excess atoms should have thermal energy $k_B T > \Delta(T)$ to penetrate the superfluid region suggests the relation between T^* and $\Delta(T)$ to be $k_B T^* \approx \Delta(T^*)$. From our experimental results, $T^* \approx 0.09 T_F$ and $\Delta(T^*) \approx h \times 3.3$ kHz.

In conclusion, we have observed phase separation of the superfluid and the normal component in a strongly interacting imbalanced Fermi gas. The shell structure consisting of a superfluid core of equal densities surrounded by a normal component of unequal densities was clearly identified using *in situ* phase-contrast imaging and 3D image reconstruction. The technique is a new method to measure the *in situ* density distribution, allowing direct comparison with theoretical predictions.

We thank G. Campbell for critical reading of the manuscript. This work was supported by the NSF, ONR, and NASA.

*Electronic address: yishin@mit.edu

[1] P. Fulde and R. A. Ferrell, Phys. Rev. **135**, A550 (1964).
[2] A. I. Larkin and Y. N. Ovchinnikov, Zh. Eksp. Teor. Fiz. **47**, 1136 (1964) [Sov. Phys. JETP **20**, 762 (1965)].
[3] G. Sarma, J. Phys. Chem. Solids **24**, 1029 (1963).
[4] W. V. Liu and F. Wilczek, Phys. Rev. Lett. **90**, 047002 (2003).
[5] M. W. Zwierlein *et al.*, Science **311**, 492 (2006).
[6] G. B. Partridge *et al.*, Science **311**, 503 (2006).
[7] M. W. Zwierlein *et al.*, Nature (London) **442**, 54 (2006).
[8] A. M. Clogston, Phys. Rev. Lett. **9**, 266 (1962).
[9] P. F. Bedaque *et al.*, Phys. Rev. Lett. **91**, 247002 (2003).
[10] J. Carlson and S. Reddy, Phys. Rev. Lett. **95**, 060401 (2005).
[11] D. E. Sheehy and L. Radzihovsky, Phys. Rev. Lett. **96**, 060401 (2006).
[12] M. W. Zwierlein and W. Ketterle, cond-mat/0603489.
[13] G. B. Partridge *et al.*, cond-mat/0605581. Partridge *et al.* state that their observations are consistent with phase separation, but that they do not prove phase separation and do not rule out other redistributions of atoms.
[14] Z. Hadzibabic *et al.*, Phys. Rev. Lett. **91**, 160401 (2003).
[15] M. W. Zwierlein *et al.*, Nature (London) **435**, 1047 (2005).
[16] C. A. Regal *et al.*, Phys. Rev. Lett. **92**, 040403 (2004).
[17] M. W. Zwierlein *et al.*, Phys. Rev. Lett. **92**, 120403 (2004).
[18] This underestimates the "true" condensate fraction since the bimodal distribution used for fitting does not account for the repulsion between the condensate and the normal components.
[19] The probe frequency was detuned by about 3 MHz from the exact center between the two resonance frequencies (frequency difference ~80 MHz, natural linewidth $\Gamma =$ 6 MHz) in order to compensate the effect of absorption, zeroing the optical signal in an equal mixture (Fig. 1).
[20] R. N. Bracewell, *The Fourier Transform and Its Applications* (McGraw-Hill, New York, 1986).
[21] T. N. De Silva and E. J. Mueller, Phys. Rev. A **73**, 051602(R) (2006).
[22] A. Imambekov *et al.*, cond-mat/0604423.
[23] W. Yi and L.-M. Duan, Phys. Rev. A **73**, 031604(R) (2006).
[24] T. Mizushima *et al.*, Phys. Rev. Lett. **94**, 060404 (2005).
[25] K. Machida *et al.*, cond-mat/0604339.
[26] C.-C. Chien *et al.*, cond-mat/0605039.
[27] J.-P. Martikainen, Phys. Rev. A **74**, 013602 (2006).
[28] M. M. Parish *et al.*, cond-mat/0605744.